

Recognition with metallo cavitands

Faiz-Ur Rahman^{a,b}, Yong-sheng Li^{a,b}, Ioannis D. Petsalakis^c, Giannoula Theodorakopoulos^c, Julius Rebek Jr.^{a,b,d,e,1}, and Yang Yu^{a,b,1}

^aCenter for Supramolecular Chemistry & Catalysis, Shanghai University, Shanghai 200444, China; ^bDepartment of Chemistry, College of Science, Shanghai University, Shanghai 200444, China; ^cTheoretical and Physical Chemistry Institute, The National Hellenic Research Foundation, Athens 11635, Greece; dSkaggs Institute for Chemical Biology, The Scripps Research Institute, La Jolla, CA 92037; and eDepartment of Chemistry, The Scripps Research Institute, La

Contributed by Julius Rebek Jr., July 19, 2019 (sent for review May 28, 2019; reviewed by Makoto Fujita and Bruce C. Gibb)

We describe here the effects of metal complexation on the molecular recognition behavior of cavitands with quinoxaline walls. The nitrogen atoms of the quinoxalines are near the upper rim of the vase-like shape and treatment with Pd(II) gave 2:1 metal:cavitand derivatives. Characterization by ¹H, ¹³C NMR spectroscopy, HR ESI-MS, and computations showed that the metals bridged adjacent quinoxaline panels and gave cavitands with $C_{2\nu}$ symmetry. Both water-soluble and organic-soluble versions were prepared and their host/guest complexes with alkanes, alcohols, acids, and diols (up to C12) were studied by ¹H NMR spectroscopy. Analysis of the binding behavior indicated that the metals rigidified the walls of the receptive vase conformation and enhanced the binding of hydrophobic and even water-soluble guests, compared to related cavitands reported previously. The results demonstrated that the conformational dynamics of the cavitand were slowed by the coordination of Pd(II) and stabilized the host's complexes.

cavitands | molecular recognition | metallo cavitand | water-soluble containers | Pd(II) stabilized cavitand

avitands are container host molecules with an open end and movable walls that allow uptake and release of guests. Since their introduction by Cram and coworkers (1) and Dalcanale et al. (2), cavitands are widely used in studies of molecular recognition and confinement. Many structural variants are available, but most involve a resorcinarene platform built up with aromatic panels as walls. These compounds exist in 2 shapes: the receptive vase shape and unreceptive kite (or velcrand) shape (Fig. 1). The velcrand shapes often exist in dimeric forms known as "velcraplexes" (3) Earlier, Diederich and coworkers (4-6) thoroughly examined the effects of temperature, pH, solvent, and metal ions on the equilibrium between these shapes of heterocyclic cavitands. These cavitands featured pyrazine and quinoxaline walls (Fig. 1) (7), and the action of Zn(II) ions prevented guest binding by stabilizing the kite forms. This work was undertaken to place Pd centers—and potentially interactive sites (8)—near the cavity (9) and its contents. Container molecule function is closely related to the dynamics of guest exchange (10), and our interest was to explore the effects of the metal on this process. Our cavitands also incorporate quinoxaline walls, but in an arrangement isomeric with those described earlier (Fig. 1). By placing the heteroatoms near the rim of the cavitands, we find that metal binding stabilizes the vase forms and enhances guest binding.

Results and Discussion

The water-soluble 1 and organic-soluble 2 cavitands with quinoxaline functionalized walls were prepared as recently reported (SI Ap*pendix*) (11). Ion exchange of Cl to NO₃ anions of 1 using *n*-butyl ammonium nitrate proceeded in >90% isolated yield. All of the cavitands could be purified by simply washing with suitable solvents and were characterized by high-resolution ¹H, ¹³C NMR spectroscopy, and mass spectrometry HR ESI-MS (SI Appendix, Figs. S1–S12).

Cavitand conformations can be readily determined by ¹H NMR spectroscopy: The vase form is recognized from its methine proton's characteristic signal observed around 5.5 ppm, whereas in the kite form the same signals are observed below 4 ppm (7, 12). Both 1 and 2 showed vase conformations in DMSO-d₆ (SI Appendix, Figs. S1 and S5) where the solvent acts as guest. The reaction of 2 with 2.2 equivalents of Pd(II) precursor complex [Pd(EDA)(CH₃CN)₂· $2BF_4$] (EDA = ethylene diamine) in DMF gave **2-Pd**. (Scheme 1 and SI Appendix, Figs. S2 and S4). Only 2 metals are bound by the cavitand, irrespective of equivalents of Pd(II) precursor complex added, the solvents used or the time of exposure (SI Appendix, Figs. S13-S23), as confirmed by high-resolution electrospray mass analysis (SI Appendix, Figs. S8-S10).

Computational methods were applied to predict the effect of metal binding on the cavitands' shapes. Geometry-optimization density functional theory calculations (13) carried out on cavitands 2 and 2-Pd, employing the B3LYP functional (14) and the def2svp basis set, provided in the Gaussian 16 suite of programs (15, 16). While 2 shows the arrangement of the walls in the expected square, chelation of Pd by adjacent walls distorts the array to a diamond shape in 2-Pd (Fig. 2 and SI Appendix, Figs. S92–S94). The distortion extends to the resorcinarene where the arrangement of aromatics moves from square to rectangular, toward a shape known in related calixarene compounds as a "pinched cone" (17). An estimate of the capacities gave 520 A^3 for 2 and 410 A^3 for 2-Pd. An arbitrary "lid" was placed at the level of the H atoms of the rim for the computations, but these are open-ended structures. The volumes are for the idealized shapes shown, yet breathing motions of the walls are expected to allow distortions that conform to a given guest. The effects of

Significance

Cavitands are nanoscale container molecules widely used in studies of molecular recognition and reactivity. They act as hosts that temporarily confine small molecule guests and much of their action as reaction chambers is due to movable walls allowing the uptake and release of guests. Water-soluble and organic-soluble cavitands featuring quinoxaline walls were prepared and their complexes with alkanes, and amphiphilic guests were characterized by ¹H NMR spectroscopy and computational methods. The quinoxalines bound Pd(II) near the rim of the cavitands and distorted the shape of the space, stabilized the receptive forms, and enhanced guest binding. Further development and application of cavitands as reaction vessels depends on closely positioned charges and potentially interactive sites near the cavity and its contents.

Author contributions: J.R. and Y.Y. designed research; F.-U.R. and Y.-s.L. performed research; I.D.P. and G.T. contributed new reagents/analytic tools; F.-U.R., J.R., and Y.Y. analyzed data; and F.-U.R., J.R., and Y.Y. wrote the paper.

Reviewers: M.F., The University of Tokyo; and B.C.G., Tulane University.

The authors declare no conflict of interest.

Published under the PNAS license

¹To whom correspondence may be addressed. Email: jrebek@scripps.edu or yangyu2017@ shu.edu.cn.

This article contains supporting information online at www.pnas.org/lookup/suppl/doi:10. 1073/pnas.1909154116/-/DCSupplemental

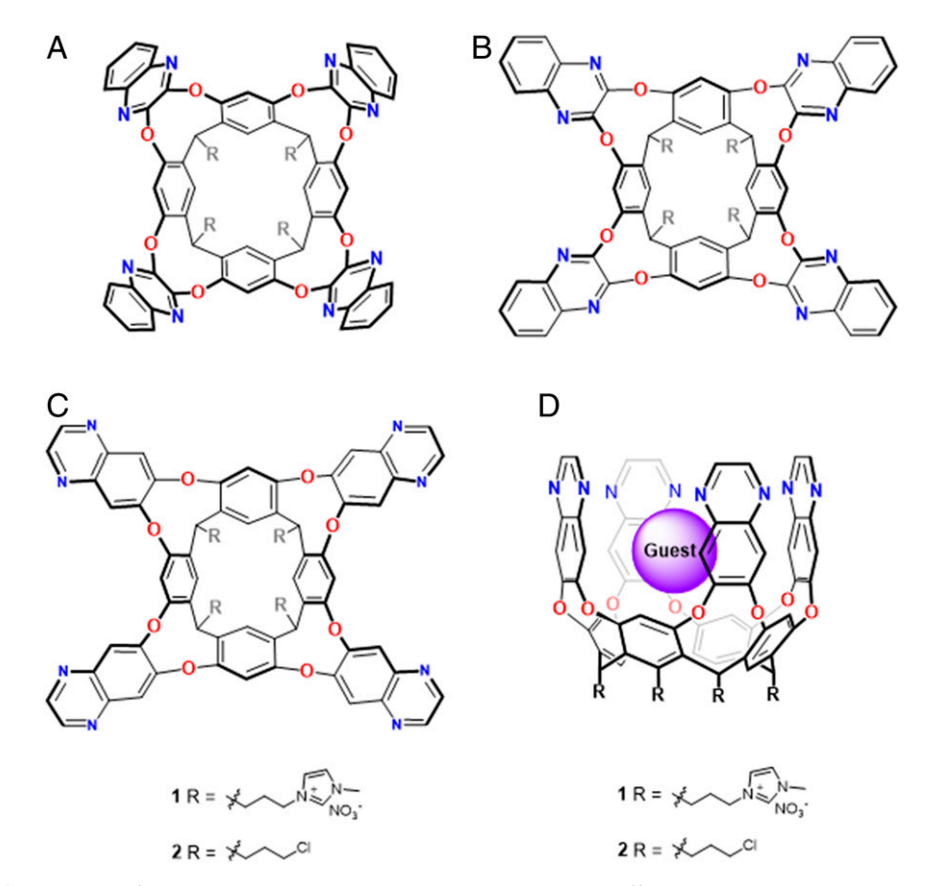


Fig. 1. (A) Vase and (B) kite shapes of earlier quinoxaline cavitands. Their interconversion is effected by solvent, temperature, metal ions, pH, and resorcinarene substitution. (C) Kite and (D) vase host/guest forms of cavitands with organic and water-soluble "feet."

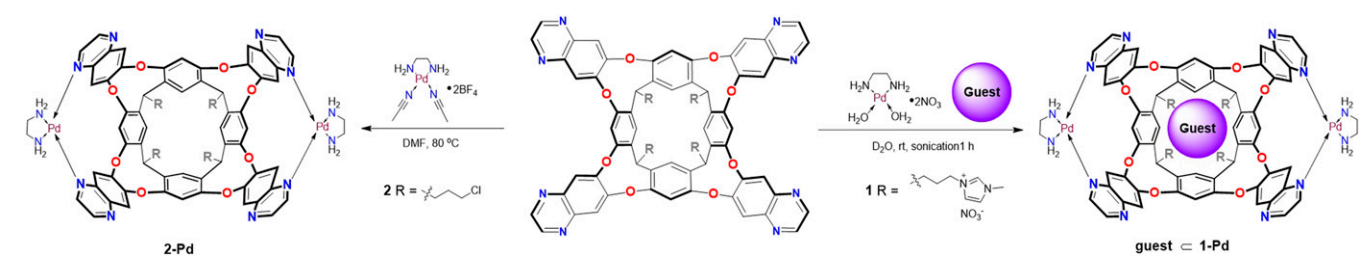
the aromatic walls on the magnetic anisotropy experienced by a nucleus placed in this environment are presently unknown but may be estimated (18).

The ¹H NMR spectra show the expected changes in the quinoxaline and the resorcin[4]arene protons as the Pd(II) precursor complex is added to **2** in organic solvents (Fig. 3 and *SI Appendix*, Figs. S2 and S4). The 4 signals in the aromatic region are split into 8 signals indicating the coordination of Pd(II) to only 1 N atom of each quinoxaline. At the same time, signals were observed in the 2.9 to 3.0-ppm region for the 2 methylenes of the coligand (EDA) (Fig. 3 and *SI Appendix*, Fig. S4). The amino group protons of the coligand were assigned at 5.6 ppm overlapped with the methine signals of the cavitand. The signals for the feet of the cavitand remained unchanged as Pd(II) coordination sites are at some distance from these positions.

The titration of 1 in DMSO- d_6 was performed using the Pd(II) precursor complex [Pd(EDA)(H₂O)₂·2NO₃](SI Appendix, Figs. S24–S28), and it showed behavior similar to 2. However, binding

experiments in D_2O where 1 exists exclusively in the kite form gave different results. Cyclopentane does not noticeably bind to 1 in D_2O (Fig. 4, bottom spectrum). But in the presence of 1 to 3 equiv. of the Pd(II) precursor, the cavitand quickly shifts to the vase conformation which takes up cyclopentane (Fig. 4 and *SI Appendix*, Figs. S29 and S30). Apparently, Pd(II) coordination stabilizes the host/guest complex, much as the covalent bonds of Gibb's (19–21) cavitand provides rigidification, stability, and a comparably hydrophobic interior.

We also treated 1 with increasing quantities of Pd(EDA)(H₂O)₂· 2NO₃ in the presence of cyclohexylcarboxylic acid, mixing all of the 3 components and sonicating for 1 h in D₂O (Scheme 1). The complex 1-Pd with cyclohexyl carboxylic acid in the cavity emerged (SI Appendix, Figs. S31–S33) and appeared to be stable indefinitely. The order of reagent combination does not matter: The binding properties of 1-Pd develop as the system self-assembles from cavitand, metal, and guest. Pd(II) coordination can make a bad guest (e.g., cyclopentane) into a good one.



Scheme 1. Route for the metallation of the cavitands: 2 equiv. of $[Pd(EDA)(CH_3CN)_2 \cdot 2BF_4]$ (EDA = ethylene diamine) in DMF gave 2-Pd (Left); 2 equiv. of $[Pd(EDA)(H_2O)_2 \cdot 2NO_3]$ and guest in water-generated complexes of 1-Pd in situ.

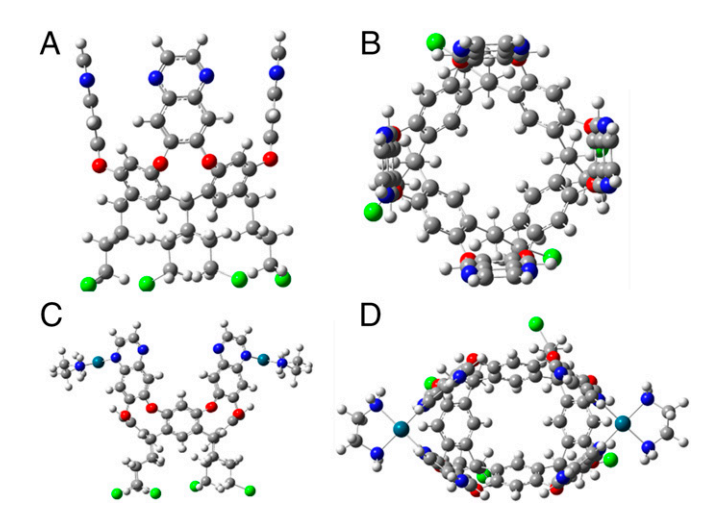


Fig. 2. Computed structures of 2 (A) side view, (B) top view and 2-Pd (C) side view, (D) top view (see Results and Discussion for details).

We examined a number of potential guests in unbuffered D_2O using the in situ method. Alkanes, alcohols, cycloalkanes, and alkanoic acids (Fig. 5) were all taken up but in somewhat different ways. Straight-chain alkanes are not bound in 1, but n-alkanes from C5 to C12 were all captured in the metalo-cavitand 1-Pd; (Fig. 6A and *SI Appendix*, Figs. S34–S42). The C5 showed a unique conformation in the space of 1-Pd, as the middle methylene protons occupied the deepest position (the furthest upfield shift) while the 2 methyl groups were directed toward the mouth of the cavity: the pentane is folded. Among these alkanes, only C6 showed the broad signals indicating guest motions occurring at an intermediate rate on the NMR chemical shift timescale. The space and shape of the cavity do not capture this guest in a single conformation.

Longer chain (>C6) alkanes and alkyl guests with polar headgroups were consistently bound in the same arrangements: the methyl groups and the next 6 carbons experienced the same magnetic environments as shown by the superimposable signal patterns in the upfield regions of their spectra (Fig. 64). For cavitands with C_{4v} symmetry, the chemical shifts correlate predictably with depth in the cavity. For example, terminal methyl groups of n-alkanes show the greatest upfield shifts ($-\Delta\delta$ ppm) as they fit into the resorcinarene bowl. Penultimate methylenes show slightly decreased shifts, and so on in a monotonic manner that indicate—on average—a given guest nucleus is equidistant from the 4 walls (22).

These gradual changes do not hold for the Pd complexes, as the change in symmetry to C_{2v} has strong effects on the shape and magnetic anisotropy of the cavity. The -CH₃ groups of alkyl chains appear at -4.5 to -4.6 ppm (corresponding to a $-\Delta\delta$ of 5.3 to 5.4 ppm) but the -CH₂-CH₃ appear at -4.2 to -4.3 ppm ($-\Delta\delta$ of 5.4 to 5.5 ppm) or deeper than the methyl groups. This is possible if the terminus is folded and fits the rectangular array of the resorcinarene aromatics. More likely, the methylenes must be closer to the walls as caused by pinching of the cavitand's corners by chelation of the Pd. The identical signal patterns (Fig. 64) provide a consistent map of chemical shifts for packed alkyl groups.

We also tested primary alcohol guests, methanol to dodecan-1-ol, as guests (Fig. 6B and SI Appendix, Figs. S43–S55). None of these compounds bind in 1 yet they gave stable host–guest complexes with 1-Pd. Only smallest methanol preferred the aqueous medium, but ethanol, propanol, and l-butanol were buried deep in the space, indicating the hydrophilic hydroxyl headgroup must be inside the hydrophobic cavity. Despite the miscibility of these alcohols with water, they were guests, showing Pd(II) coordination rigidifies the walls and stabilizes the complexes. The series from 1-pentanol to dodecanol indicates a linear binding similar to n-alkane guests but with the terminal OH outside the cavity.

Aliphatic acids also followed the trend of alcohols and bound well in **1-Pd** (Fig. 6C and SI Appendix, Figs. S56–S67). Acetic acid showed weak binding (the host–guest ratio is >1:1) and involves rapid exchange of the guest between cavitand and the bulk water solvent (Fig. 6C and SI Appendix, Fig. S57). Small-size acids from propanoic acid to hexanoic acid bind in a way that the carboxyl group also remained inside the cavity of **1-Pd**. For longer acids from heptanoic acid to dodecanoic acid we observed 6 carbons of the chain bound in a manner similar to the alkane guests.

The binding behavior of aliphatic α,ω diols gave unexpected results. In other water-soluble cavitands, α,ω dipolar guests show folded conformations (if they bind at all) with the polar groups exposed. For shorter chain diols (2 to 6 carbons) broad chemical shifts were observed in **1-Pd** for the methylene protons showing intermediate exchange rates (Fig. 6D and SI Appendix, Figs. S68–S79). For longer chains (7 to 12 carbons) the number of signals requires the insertion of 1 terminal OD group in the depths of the hydrophobic cavity. The methylenes bind in a linear manner resembling the alkanes with up to 6 methylenes of the carbon chain inside. Additional methylenes and the O-D at other terminal were outside

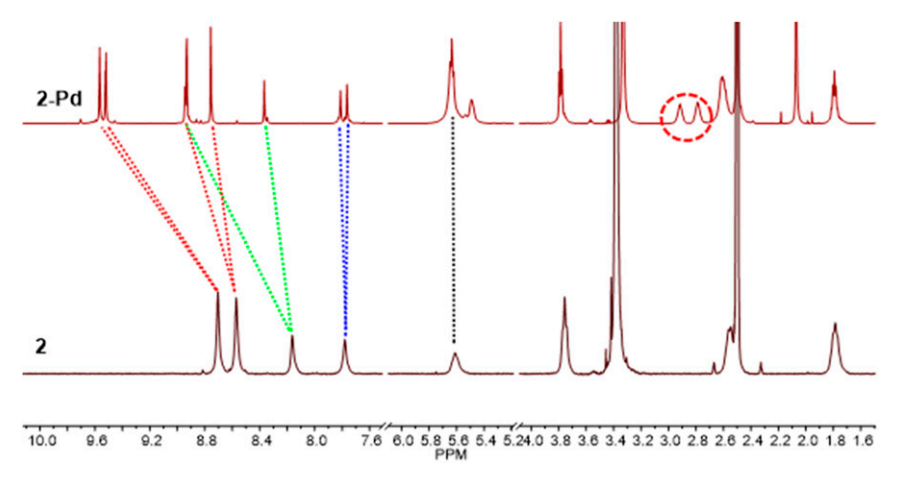


Fig. 3. Comparative ¹H NMR spectra of 2 and 2-Pd. The red circle represents ethylene diamine signals (coligand) in 2-Pd. Black dotted line indicates the methine protons, blue and green lines represent the resorcinarene protons, and the red lines represent the quinoxaline protons of 2 (shifted downfield in 2-Pd). Free CH₃CN molecules were generated on the coordination of Pd(II) complex with 2.

Rahman et al. PNAS Latest Articles | 3 of 6

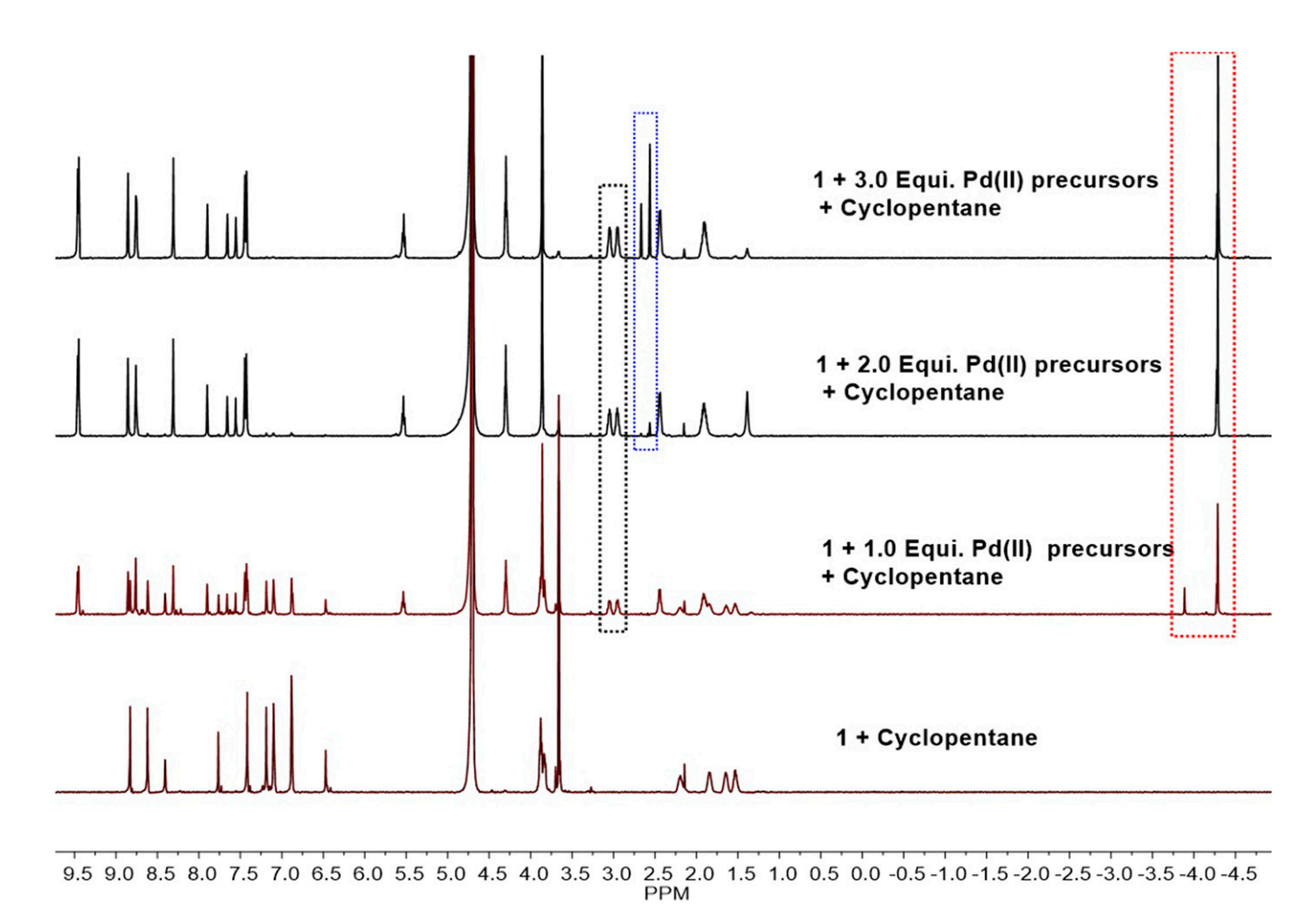
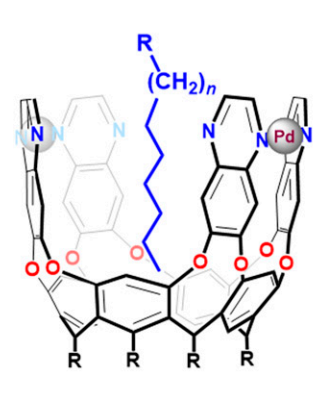


Fig. 4. Comparative 1H NMR spectra plot of 1+ excess of cyclopentane and increasing equivalent quantity (0-3.0) of Pd(EDA)(H_2O)₂·2NO₃ after 1 h sonication in D₂O at room temperature. The red rectangle contains the signal of the bound cyclopentane, the blue rectangle encloses those of the free Pd(EDA)(H_2O)₂·2NO₃, and the black rectangle encloses signals of Pd(EDA)(H_2O)₂·2NO₃ coordinated to 1.

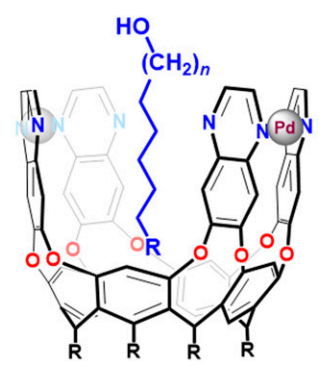
in the bulk aqueous medium. Because of the exchange of OH to OD in D_2O , the RO-D signal is not observed in the 1H NMR spectrum.

Cyclic alkanes and amphiphilic carboxylic acids also showed strong binding in **1-Pd** (Fig. 7 and *SI Appendix*, Figs. S80–S91). Cyclopentane and cyclohexane all gave well-resolved spectra of 1:1

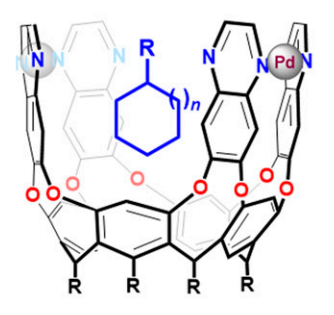
complexes. In the case of cycloheptane, an additional smaller peak at -3.27 ppm was observed (Fig. 7A and SI Appendix, Fig. S83). This is likely due to the rupture of the Pd bridges, since cyclooctane and cyclodecane binding with **1-Pd** gave the same spectra as their binding in **1** alone (11) (Fig. 7A and SI Appendix, Figs. S80–S85).



R = H, *n*-pentane to dodecane; R = COOH, Acetic acid to dodecanoic acid



R = H, Methanol to dodecan-1-ol; R = OH, Ethanediol to 1,12-dodecanediol



R = H, cyclopentane to cyclooctane and cyclodecane ; R = COOH, cyclopentanecarboxylic acid to cycloheptanecarboxylic acid

Fig. 5. Cartoons of the complexes of 1-Pd and n-alkanoic acids, n-alkanoic acids, n-alkanoids, α_n -n-alkanoids, cycloalkanes, and cyclic alkanoic acids. The long-chain compounds are positioned linearly in the cavity, cycloakanes tumble rapidly, and cyclic acids are fixed with the carboxyl groups exposed to solvent D_2O .

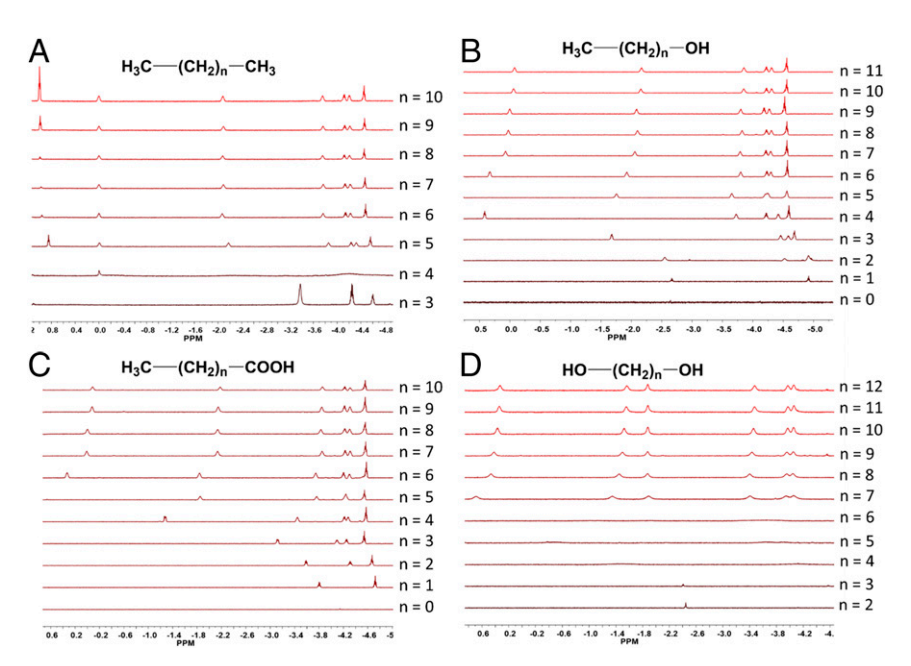


Fig. 6. Partial ¹H NMR spectra of the complexes formed between 1-Pd and excess of guest; (A) n-alkanes, (B) n-alcohols, (C) n-alkanoic acids, and (D) α , α n-alkanediols in D_2O .

These larger guests are not accommodated by the space: they force the pinched quinoxaline walls further apart and rupture the Pd chelation; hydrophobicity trumps metal coordination.

Various carboxylic acids, even those with good water solubility were taken up by **1-Pd** (Fig. 7*B* and *SI Appendix*, Figs. S86–S91). Again, the larger sizes (e.g., cycloheptylcarboxylic acid) do not fit inside **1-Pd** and the complexes reverted to those of the guest inside **1** alone. (*SI Appendix*, Fig. S91).

All of the cycloalkane guests showed sharp, single lines for their spectra (Fig. 7A), indicating that the guests rotate rapidly (on the NMR chemical shift timescale) on all 3 axes within the host. Also, internal dynamics of the guests (e.g., ring flipping) are fast on this timescale. Free cyclohexane's resonance is ~ 1.40 ppm and cyclohexane bound in 1 is observed at -3.34 ppm (11), so the square arrangement of walls induces an upfield shift, $\Delta \delta = -4.74$ ppm, as a time-averaged value for all of the guest's hydrogens. Within 1-Pd, cyclohexane's resonance is

at -4.0 ppm or $\Delta\delta = -5.4$ ppm. Cyclopentane has even a larger value at -4.3 ppm ($\Delta\delta = -5.8$ ppm) (*SI Appendix*, Figs. S81 and S82). The higher aromatic walls of 1 and 1-Pd compared with the earlier cavitands (i.e., $\Delta\delta = -3.58$ ppm) (23) offer more shielding (24) and are the likely sources of the larger guest upfield shifts. The closer quinoxaline walls and the distorted resorcinarene cavity of 1-Pd also contribute to the increased magnetic anisotropy.

Outlook

The coordination of Pd(II) in the walls of a quinoxaline cavitand induces conformational change from kite to vase and enhances guest binding. Complexation of more water-soluble and amphiphilic guests could be achieved. Unlike the more dynamic water-soluble cavitands reported previously, the Pd(II)-based cavitands showed binding properties for small organic molecule guests such as alkanes, alkanols, alkanoic acids, cyclic alkanes, and

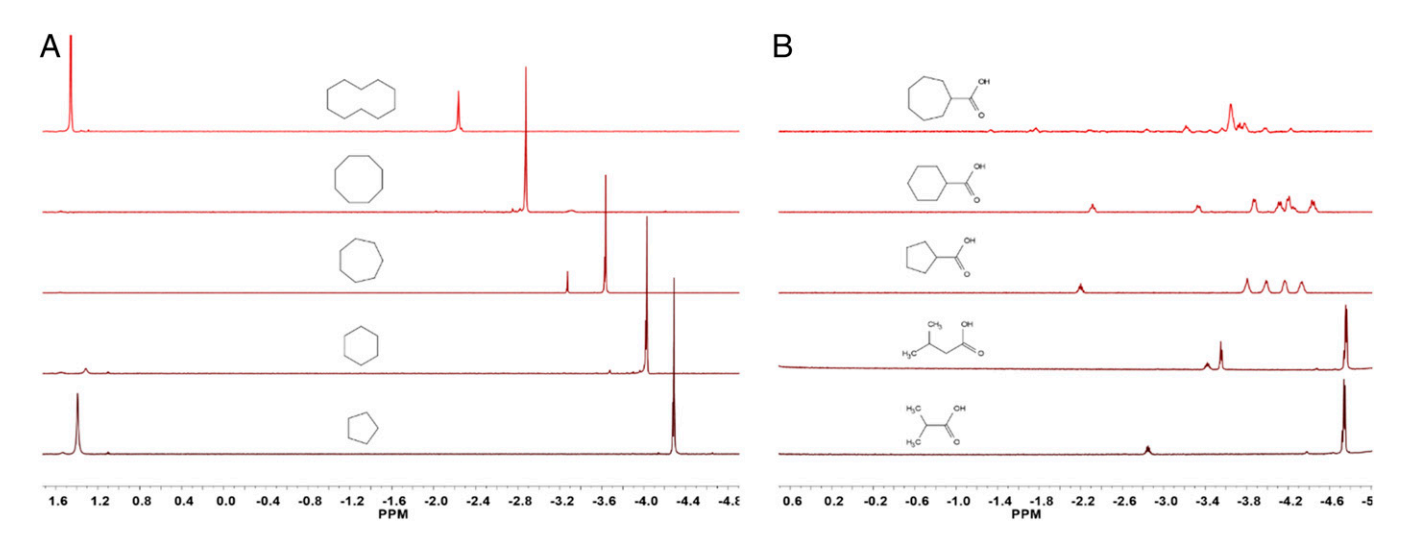


Fig. 7. Partial ¹H NMR spectra of the complexes formed between 1-Pd and excess guests in D₂O. (A) Cycloalkanes, (B) branched chain alkanoic acids and cycloalkyl carboxylic acids.

Rahman et al. PNAS Latest Articles | 5 of 6

cyclic carboxylic acids augur well for applications in smallmolecule sensing and recognition. The direct contact between the guest and metal is unlikely, but nearby charges are known to have profound effects on the stabilization of intermediates (25) and the course of reactions (26) inside containers (27). Metallo-cages have also found applications in the solid-state structural analysis of bound guests (28–31). The binding of Pd to cavitands reported here reorganizes the shape of the space and offers selectivities in guest binding that will be reported in due course.

ACKNOWLEDGMENTS. This work was supported by the National Natural Science Foundation of China (Grant 21801164), the US National Science Foundation (CHE 1801153). and by Shanghai University (N.13-G210-19-230), Shanghai, China. Y.Y. thanks the Program for Professor of Special Appointment (Dongfang Scholarship) of the Shanghai Education Committee.

- 1. J. R. Moran, S. Karbach, D. J. Cram, Cavitands: Synthetic molecular vessels. J. Am. Chem. Soc. 104, 5826-5828 (1982).
- 2. E. Dalcanale, P. Soncini, G. Bacchilega, F. Ugozzoli, Selective complexation of neutral molecules in organic solvents. Host-quest complexes and cavitates between cavitands and aromatic compounds, J. Chem. Soc. Chem. Commun., 500-502 (1989)
- 3. D. J. Cram, H. J. Choi, J. A. Bryant, C. B. Knobler, Solvophobic and entropic driving forces for forming velcraplexes, which are 4-fold, lock-key dimers in organic media. J. Am. Chem. Soc. 114, 7748-7765 (1992).
- 4. P. J. Skinner, A. G. Cheetham, A. Beeby, V. Gramlich, F. Diederich, Conformational switching of resorcin[4]arene cavitands by protonation, preliminary communication. Helv. Chim. Acta 84, 2146-2153 (2001).
- V. A. Azov, B. Jaun, F. Diederich, NMR investigations into the vase-kite conformational switching of resorcin[4]arene cavitands. Helv. Chim. Acta 87, 449-462 (2004).
- 6. M. Frei, F. Marotti, F. Diederich, Zn(II)-induced conformational control of amphiphilic cavitands in langmuir monolayers. Chem. Commun. (Camb.), 1362-1363 (2004).
- 7. P. Roncucci et al., Conformational behavior of pyrazine-bridged and mixed-bridged cavitands: A general model for solvent effects on thermal "vase-kite" switching. Chemistry 12, 4775-4784 (2006).
- 8. T. Iwasawa, Recent developments of cavitand-recessed type metal catalysts. Tetrahedron Lett. 58, 4217-4226 (2017).
- S. Korom, P. Ballester, Attachment of a Rull complex to a self-folding hexaamide deep cavitand, J. Am. Chem. Soc. 139, 12109-12112 (2017).
- 10. L. Escobar, D. Villarón, E. C. Escudero-Adán, P. Ballester, A mono-metallic Pd(ii)-cage featuring two different polar binding sites. Chem. Commun. (Camb.) 55, 604-607 (2019).
- F.-U. Rahman, H.-N. Feng, Y. Yu, A new water-soluble cavitand with deeper guest binding properties. Org. Chem. Front. 6, 998-1001 (2019).
- 12. K. D. Zhang, D. Ajami, J. Rebek, Hydrogen-bonded capsules in water. J. Am. Chem. Soc. 135, 18064-18066 (2013).
- A. D. Becke, Density-functional thermochemistry. III. The role of exact exchange. I. Chem. Phys. 98, 5648-5652 (1993).
- 14. F. Weigend, R. Ahlrichs, Balanced basis sets of split valence, triple zeta valence and quadruple zeta valence quality for H to Rn: Design and assessment of accuracy. Phys. Chem. Chem. Phys. 7, 3297-3305 (2005).
- 15. K. Wolinski, J. F. Hinton, P. Pulay, Efficient implementation of the gauge-independent atomic orbital method for NMR chemical shift calculations. J. Am. Chem. Soc. 112, 8251-8260 (1990).
- 16. M. J. Frisch et al., Gaussian 16, Revision B.01 (Gaussian, Inc., Wallingford, CT, 2016).

- 17. M. Conner, V. Janout, S. L. Regen, Pinched-cone conformers of calix 4 arenes. J. Am. Chem. Soc. 113, 9670-9671 (1991).
- 18. P. V. R. Schleyer, C. Maerker, A. Dransfeld, H. Jiao, N. J. R. van Eikema Hommes, Nucleus-independent chemical shifts: A simple and efficient aromaticity probe. J. Am. Chem. Soc. 118, 6317-6318 (1996).
- 19. J. H. Jordan, B. C. Gibb, Molecular containers assembled through the hydrophobic effect, Chem. Soc. Rev. 44, 547-585 (2015).
- 20. C. L. Gibb, B. C. Gibb, Well-defined, organic nanoenvironments in water: The hydrophobic effect drives a capsular assembly. J. Am. Chem. Soc. 126, 11408-11409 (2004).
- 21. S. Liu, B. C. Gibb, High-definition self-assemblies driven by the hydrophobic effect: Synthesis and properties of a supramolecular nanocapsule. Chem. Commun. (Camb.), 3709-3716 (2008)
- 22. Y. Yu, K.-d. Zhang, I. D. Petsalakis, G. Theodorakopoulos, J. Rebek, Asymmetric binding of symmetric guests in a water-soluble cavitand. Supramol. Chem. 30, 473-478 (2018)
- 23. H.-N. Feng, M. Petroselli, X.-H. Zhang, J. J. Rebek, Y. Yu, Cavitands: Capture of cycloalkyl derivatives and 2-methylisoborneol (2-MIB) in water. Supramol. Chem. 31, 108-113
- 24. G. Peñuelas-Haro, P. Ballester, Efficient hydrogen bonding recognition in water using aryl-extended calix[4]pyrrole receptors. Chem. Sci. 10, 2413-2423 (2018).
- 25. M. Ziegler, J. L. Brumaghim, K. N. Raymond, Stabilization of a reactive cationic species by supramolecular encapsulation. Angew. Chem. Int. Ed. Engl. 39, 4119-4121 (2000).
- 26. K. Wang et al., Electrostatic control of macrocyclization reactions within nanospaces. J. Am. Chem. Soc. 141, 6740-6747 (2019).
- 27. M. Yoshizawa, M. Tamura, M. Fujita, Diels-alder in aqueous molecular hosts: Unusual regioselectivity and efficient catalysis. Science 312, 251-254 (2006).
- 28. S. Yoshioka, Y. Inokuma, M. Hoshino, T. Sato, M. Fujita, Absolute structure determination of compounds with axial and planar chirality using the crystalline sponge method. Chem. Sci. 6, 3765-3768 (2015).
- 29. M. Fujita, M. Tominaga, A. Hori, B. Therrien, Coordination assemblies from a Pd(II)cornered square complex. Acc. Chem. Res. 38, 369-378 (2005).
- 30. M. Kawano, Y. Kobayashi, T. Ozeki, M. Fujita, Direct crystallographic observation of a coordinatively unsaturated transition-metal complex in situ generated within a selfassembled cage. J. Am. Chem. Soc. 128, 6558-6559 (2006).
- 31. Y. Hatakeyama, T. Sawada, M. Kawano, M. Fujita, Conformational preferences of short peptide fragments. Angew. Chem. Int. Ed. Engl. 48, 8695-8698 (2009).